

Genetic resources resistant to black spot (*Alternaria alternata*) identified from Chrysanthemum-related genera and potential underlying mechanisms

Qingling Zhan , Wenjie Li, Ye Liu, Shuang Zhao, Sumei Chen, Weimin Fang, Fadi Chen and Zhiyong Guan*

State Key Laboratory of Crop Genetics and Germplasm Enhancement / Key Laboratory of Flower Biology and Germplasm Innovation, Ministry of Agriculture and Rural Affairs / Key Laboratory of Biology of Ornamental Plants in East China, National Forestry and Grassland Administration / College of Horticulture, Nanjing Agricultural University, Nanjing 210095, China

* Corresponding author, E-mail: guanzhy@njau.edu.cn

Abstract

Chrysanthemum black spot disease caused by *Alternaria alternata* infestation is a widespread and extremely destructive foliar disease of chrysanthemums. We compared the resistance of 14 chrysanthemum relatives to chrysanthemum black spot disease, and identified the main indicators for the evaluation and screening of chrysanthemum disease resistance, which is of great significance in laying the foundation for a larger-scale screening of chrysanthemum relatives for disease resistance and the breeding of new disease-resistant cultivars. After artificial inoculation and identification, two disease-resistant germplasm resources, 11 moderately resistant materials, and one sensitive material were obtained. In both resistant and susceptible species, we found that the trichome density and leaf wax content of the resistant material were significantly higher than that of the sensitive material, while the stomata size was smaller than that of the sensitive material. In addition, we found that the leaf extract of the disease-resistant germplasm effectively inhibited the growth rate of *A. alternata* mycelium on the plate, and GC-MS components found that the leaves of resistant germplasm contained more volatile antifungal organic compounds, of which the abundant falcarinol and Germacrene D might play an important role in resistance to chrysanthemum black spot disease. In summary, epidermal trichome density, wax content and terpene substance content are three important reference indicators for disease resistance evaluation of related genera of chrysanthemum. The identified resistant germplasm can also be used as parents for future cross-breeding or as rootstocks.

Citation: Zhan Q, Li W, Liu Y, Zhao S, Chen S, et al. 2024. Genetic resources resistant to black spot (*Alternaria alternata*) identified from Chrysanthemum-related genera and potential underlying mechanisms. *Ornamental Plant Research* 4: e001 <https://doi.org/10.48130/opr-0023-0023>

Introduction

Chrysanthemum is one of the most widely cultivated flowers worldwide due to its outstanding ornamental, medicinal, and beverage value. However, in chrysanthemum planting areas, it is easy to be infected by bacteria and fungi, which induces various diseases, among which black spot disease caused by *Alternaria alternata* is one of the main diseases of chrysanthemum. Chrysanthemum black spot disease (hereafter referred to as CBS) causes black spots on the leaves, stunted plants, reduced flower production and quality, and in severe cases the whole plant withers and dies, so this causes huge economic losses to chrysanthemum growers and companies. As far as we know, pesticide residues and environmental degradation can result from applying pesticides as a traditional method of disease management. Screening and cultivating resistant germplasm of chrysanthemums is a friendly way to control CBS. Resistant germplasm can be used as parents of chrysanthemum hybrid breeding and rootstock of chrysanthemum asexual propagation. Previous studies have shown that chrysanthemum-related genera (abbreviated as CRG below) usually hold excellent resistance, including tolerance to salt^[1, 2], drought^[3, 4], waterlogging^[5], heat^[6], heavy metals^[7], insect resistance^[8], and fungal suppression^[9, 10], among other things. The lack of excellent germplasm resources for disease tolerance continues to

be a constraint for disease resistance breeding, and disease resistance screening in CRG is still insufficient.

As we know, the main defense mechanisms of plants against diseases are physical and chemical defenses, among which physical defense mechanisms include trichomes, stomata, and a waxy layer. Trichomes were special structural appendages developed from plant epidermal cells, which produced a role in plant defense against biotic and abiotic stresses and were closely related to plant disease resistance^[11]. Stomata were the main channels of contact between plants and the outside world, and their density, size, and aperture also affect the successful invasion of pathogenic bacteria and are closely related to plant disease resistance^[12, 13]. For example, research revealed that trichome density and stomata density were possible contributors to willow rust resistance^[14]. Wax was a class of secondary metabolites that evolved during the long-term ecological adaptation of plants and was widely involved in plant responses to biotic stress and abiotic physiological processes^[15–17]. The epicuticular wax layer functions as a physical barrier against abiotic stresses and biotic stresses caused by pathogens or pests^[18].

Plant secondary metabolites were the chemical defense factors of plants against pathogen infection, and there were many types of them. There were three major classes of plant antimicrobial secondary metabolites: terpenoids, phenolic, and

nitrogenous compounds^[19]. Secondary metabolites could perform as biochemical fortresses to ward off pathogen invasion in plant disease resistance, in addition to functioning as signaling substances in the signal transduction of plant disease resistance^[20–22]. A previous study indicated that terpenoids were the main compounds in chrysanthemum leaves^[23].

Previous research has examined the connection between leaf physical defense structures and resistance to black spot in 17 chrysanthemum cultivars^[24]. Another study found that volatile terpenoids released from cultivated chrysanthemum leaves increased after being infested by pathogenic fungi^[25]. However, there has been inadequate exploration of germplasm with superior resistance to black spot in CRG. Moreover, the relationship between their physical and chemical defense mechanisms and disease resistance remains unclear.

We employed two artificial inoculation techniques to assess the resistance of 14 CRG against black spot disease and investigate the resistance mechanisms. Our study showed that in vitro leaf inoculation is a dependable and effective method for quickly evaluating the resistance of chrysanthemum plants against black spot disease. Additionally, we observed distinct differences in leaf structure between tolerant germplasm and susceptible germplasm. Further analysis of volatile substances in the leaves demonstrated that disease-resistant germplasm exhibited stronger antifungal properties, which were characterized using GC-MS (Gas chromatography-mass spectrometry) analysis to identify the composition of these volatile substances. These results contribute valuable germplasm resources for the future breeding of disease-resistant chrysanthemums.

Materials and methods

Plant materials and inoculation treatment

The experimental plant materials were obtained from the 'China Chrysanthemum Germplasm Resource Conservation Center' of Nanjing Agricultural University, and the species names and classifications are shown in [Supplemental Table S1](#) and [Supplemental Fig. S1](#). The rooted seedlings were cultured in a 3:1 vermiculite mixture. Seedlings were grown in long-day conditions (16 h light, 25 °C, relative humidity 75%)^[26, 27]. Plants with uniform growth were randomly divided into two groups (n = 15): the control group and the treatment group. The strain (*A. alternata*) used in the study was isolated in our laboratory from leaves with typical symptoms of CBS. The leaf inoculation was carried out as previously described^[27]. The fungus used for inoculation was grown in potato dextrose broth (PDB) medium at 28 °C shaking at 200 rpm for 24 h. Then 2 mL of mycelial fluid was inoculated on the back of the third fully expanded leaf of the plant, one leaf per plant and two loci. The inoculated leaves were covered with a ziplock bag, and the control group was inoculated with PDB. After inoculation was completed, the plants were placed in dark conditions at a temperature of 28 °C and 80% humidity for 48 h.

At the same time, we used the method of inoculation with detached leaves. The simplified detached leaf inoculation assay was the same as previous. We chose the third fully expanded leaf of a fresh and healthy plant, rinsed with sterile water and wrapped with moistened skim cotton on the petiole area, then the leaf was placed in a clean Petri dish and inoculated as described previously. After the inoculation was completed, the

plants were sealed with plastic wrap and cultured in the dark for 7 d.

Disease statistics

The severity of disease was divided into 0~3 levels: leaf health, no disease for level 0, lesion area accounted for less than 25% of the leaf for level 1, lesion area accounted for 25% to 50% of the leaf for level 2, lesion area accounted for more than 50% of the leaf for level 3. Counted the number of incidences at each level and calculated the incidence and disease index (DSI) for each species.

$$\text{Incidence (\%)} = \frac{\text{The number of diseased plants}}{\text{Total number of plants treated}} \times 100$$

$$\text{DSI} = \frac{\sum (\text{Disease grade} \times \text{Number of infected plants})}{\text{The highest disease grade} \times \text{The total number of inoculated plants}}$$

Disease resistance evaluation levels were classified according to DSI, with DSI = 0 for immunity (I), $0 < \text{DSI} \leq 30$ for resistance (R), $30 < \text{DSI} \leq 50$ for moderate resistance (MR), and $\text{DSI} > 50$ for susceptibility resistance (S).

Observation of leaf lower epidermis structure

To investigate the variation in physical defenses between resistant and sensitive materials, we examined the trichomes and stomata present on the lower epidermis of leaves. We selected the second fully grown fresh leaf below the upper portion of the plant and cut it at the same spot on both sides of the main vein, resulting in an area of approximately 3 mm². Next, we treated the leaf with a 2.5% glutaraldehyde fixative to preserve it, and stored it in a refrigerator at 4 °C after leaving it at room temperature for 2 h. The samples were then observed and photographed using scanning electron microscopy (SU8100, 3.0 kV, SEM). We analyzed three leaves for each material, with six fields of view examined for each leaf.

Determination of leaf wax content

We investigated the role of leaf wax by measuring the quantity of wax in the leaves. We determined the wax content (mg/g) in the fresh leaves by accurately weighing each plant's fresh leaves. Then, we cut the leaves and soaked them in 10 mL of chloroform for 2 min. The resulting solution was filtered into a beaker with a known weight. After the chloroform evaporated, we reweighed the leaves and subtracted the weight of the beaker to calculate the wax content (mg/g) in the fresh leaves. We repeated this process 20 times for each material and recorded the average value.

Extraction of leaf metabolites

The second or third fully expanded fresh leaf below the tip of the plant was taken, and five plants were mixed and sampled three times, for a total of 15 plants. Each 0.2 g of the freshly ground sample was added with 1 mL of ethyl acetate solution, vortexed and mixed, and then shaken in a shaker at 28 °C and 200 rpm/h for 1 h. The upper clear liquid was selected as the material to be used^[28].

Determination of antifungal activity

At a temperature of approximately 50 °C, 500 µL of the extract was placed in an unconsolidated Potato Dextrose Agar (PDA) medium. The concentration of the preparation was extracted : PDA = 1:200. After mixing, the extract was poured into a sterile Petri dish for solidification. Next, the fungal blocks were picked and placed in the middle of the treated PDA medium, and the test was conducted with PDA medium with ethyl acetate (control 2) and blank treatment (control 1) as the

control, with 15 sample sizes set for each treatment. The mycelial extension diameter (cm) was counted after 4 d and photographed and recorded.

$$\text{Inhibition rate (\%)} = \frac{(\text{Colony diameter of control 2} - \text{Treated colony diameter of extract})}{\text{Colony diameter of control 2}} \times 100\%$$

Determination of antifungal activity of Germacrene D

Rapid injection of 500 µL of ethyl acetate (containing 0.002% ethyl nonanoate as an internal standard) was performed into a 250 mg vial of Germacrene D. The vial was quickly wrapped with a sealing film and shaken to mix well, and the mother liquor was prepared for use. Take 20 µL of the mother liquor into a brown bottle containing 200 µL of ethyl acetate, mix well and seal it as the reagent to be used.

After placing the bacterial plots in the centre of the plate, 200 µL of the prepared Germacrene D reagent was sucked up and applied onto the PDA plate with the help of an applicator stick, avoiding the fungus plots when applying the reagent; the PDA plate coated with ethyl acetate was used as the control; five replicates were set for each treatment. The prepared plates were incubated in the dark at 28 °C in a light incubator, and the mycelial growth diameter was measured after 7 d.

GC-MS analysis

The sample preparation and extraction of leaf metabolites were the same. For each sample, 0.2 g of fresh leaf sample was mixed with 1 mL of ethyl acetate solution containing 0.002% nonyl acetate as an internal standard. The analysis was performed using a GC-MS system equipped with an HP-5 capillary column (30 m × 0.25 mm × 0.25 µm, Agilent Technologies, USA) and a 7000 D mass spectrometer (Agilent Technologies, USA). The carrier gas for gas chromatography was high-purity helium (He2, 99.999%), with a flow rate of 1 mL/min. The injection was performed using a 40:1 split injection with an injection temperature of 250 °C. Both liquid extraction and solid-phase microextraction (SPME) were used without splitting. The temperature gradient was set at a rate of 20 °C/min, starting from 40 °C and ramping up to 260 °C, followed by a 5-min hold at 260 °C. The cycle time optimization was performed using rapid cooling. The ionization mode of the mass spectrometer was electron ionization (EI), with an ionization voltage of 70 eV. The ion source temperature was set at 230 °C, and the ion source excitation energy was 70 eV. The solvent delay was 3 min. The GC-MS interface temperature was set at 260 °C, and the mass spectrometry analysis was performed in full-scan mode, with a mass scanning range of 20 to 500 atomic mass units (amu). The total time required for a single sample analysis was 40 min. The instrument was equipped with an automatic sample injector, and the injection volume was 100 µL.

Data processing and analysis

The area of each lesion was measured using Image J, and data analysis was performed with SPSS 26 software. These data were integrated and visualized using the R programming language and GraphPad Prism 8.0. The qualitative analysis of volatile organic compounds (VOCs) was identified by comparing the retention times of substances in the NIST (National Institute of Standards and Technology) mass spectrometry database and the mass spectra of the standards, the quantification was based on the peak area of the mass spectra.

Results

Differences in resistance to black spot disease among 14 germplasms

For disease assays, simplified detached leaf inoculation assay and whole plant inoculation assay were performed. We divided the 14 germplasms into resistant (R), moderately resistant (MR), and sensitive (S) according to the disease index. The results of identification using *in vitro* leaf inoculation were listed in Table 1. The statistical results after 7 d of inoculation showed that *C. japonese* was a resistant material (DSI = 24). Eleven germplasms, including *C. ornatum* and *A. vulgaris*, were identified as MR. Meanwhile, *A. vulgaris* Variegata, and *A. pacificum* had disease indices of 55 and 57, respectively, and were both identified as S. With the prolongation of the inoculation time, the area of the lesion continued to expand, and the lesion spreading speed of susceptible germplasms were much faster than that of resistant germplasms (Fig. 1a).

The results of identification using whole plant inoculation are shown in Table 2. We performed two independent replicates, at the same time, and the correlation coefficient was 0.974** (** means $p < 0.01$) which suggested good reproducibility. Typical disease symptoms appeared 2 d after plant inoculation (Fig. 1b). Based on the results of the DSI division, two germplasms with 'disease resistance' grade were obtained as *C. japonese* and *A. parviflora*. Meanwhile, 11 'moderately resistant' germplasms including *A. japonica* and *A. vulgaris*, etc. *A. pacificum* were still susceptible. *A. pacificum* had the largest average spot area percentage among the test materials, with a mean value of 42.7%, followed by *A. vulgaris* Variegata, with an average spot area percentage of 20.5%. The top three with a smaller proportion of lesion area were *A. japonica*, *A. parviflora*, and *C. japonese*, which were 4.2%, 5.7%, and 6.6%, respectively. Although *A. japonica* has the smallest mean lesion area percentage, it is not the most resistant.

Comparing the results above of the isolated leaf identification and plant inoculation identification, it can be seen that the agreement of the two results was very good, with a Pearson correlation coefficient for the ratios of 0.872** (** means that $p < 0.01$, data not shown). Combining the two methods, *C. japonese* and *A. parviflora* were identified as R, 11 germplasms such as *A. japonica*, *C. ornatum*, *A. vulgaris*, *A. vulgaris* Variegata as MR, *A. pacificum* as S.

Table 1. Evaluation of disease resistance after inoculation of isolated leaves of CRG.

Name	Incidence rate (%)	Percentage of spot area (%)	Disease index (DSI)	Resistance type
<i>C. japonese</i>	73	5.9	24	R
<i>C. ornatum</i>	100	6.7	33	MR
<i>A. vulgaris</i>	100	6.2	33	MR
<i>A. leucophylla</i>	100	7.5	33	MR
<i>A. parviflora</i>	100	16.2	33	MR
<i>A. rubripes</i>	100	15.1	33	MR
<i>A. annua</i>	100	16.0	33	MR
<i>A. sieversiana</i>	100	18.4	33	MR
<i>A. indices</i>	100	24.1	33	MR
<i>A. viridisquama</i>	100	19.3	33	MR
<i>A. yunnanensis</i>	100	26.6	33	MR
<i>A. japonica</i>	100	22.3	36	MR
<i>A. vulgaris</i> Variegata	100	30.7	55	S
<i>A. pacificum</i>	100	52.8	57	S

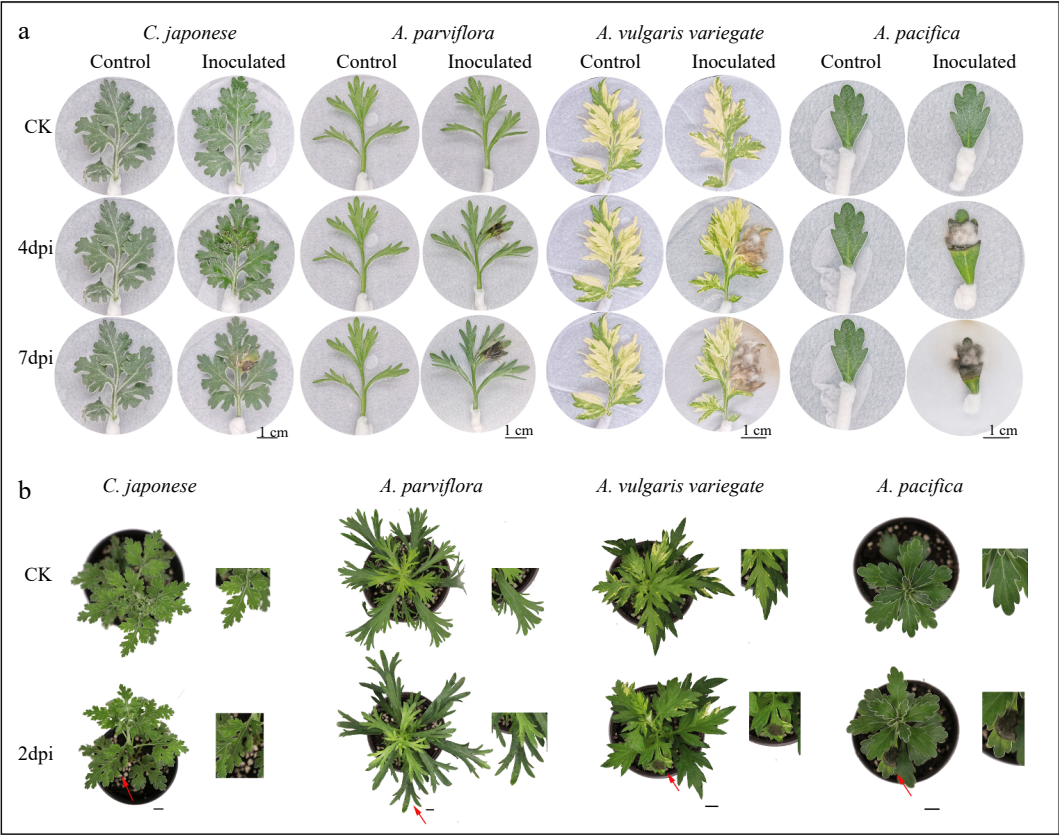


Fig. 1 Differences in disease phenotype of different plants after inoculation. From left to right: the disease degree of leaves deepens. n = 15. (a) Disease symptoms on 4 and 7 d after inoculation of isolated leaves. (b) Disease symptoms of whole plants at post 2 d inoculation. Scale bar = 1 cm.

Table 2. Evaluation of disease resistance after inoculation of whole plants of CRG.

Name	EXP 1		EXP 2		Average percentage of spot area (%)	Average DSI	Resistance type
	Incidence rate (%)	DSI	Incidence rate (%)	DSI			
<i>C. japonese</i>	83	28	92	30	6.6	29	R
<i>A. parviflora</i>	100	32	83	28	5.7	30	R
<i>A. japonica</i>	92	31	100	33	4.2	32	MR
<i>A. vulgaris</i>	100	33	100	33	6.9	33	MR
<i>A. leucophylla</i>	100	33	100	33	15.4	33	MR
<i>A. rubripes</i>	100	33	100	33	10.4	33	MR
<i>A. yunnanensis</i>	100	33	100	33	12.1	33	MR
<i>A. indices</i>	100	33	100	33	19.2	33	MR
<i>A. viridisquama</i>	100	33	100	33	20.1	33	MR
<i>A. sieversiana</i>	100	33	100	33	18.0	33	MR
<i>A. annua</i>	100	36	100	36	18.8	36	MR
<i>C. ornatum</i>	100	40	100	38	16.1	39	MR
<i>A. vulgaris Variegata</i>	100	42	100	44	20.5	43	MR
<i>A. pacificum</i>	100	62	100	57	42.7	60	S

Differences in leaf epidermis structure of resistant and susceptible germplasms

The results of resistance identification prompted us to explore the defense mechanism of plant disease resistance. Therefore, we selected three typical species for further analysis of leaf lower epidermis structure, namely stress resistant (*C. japonese*, abbreviated as R1 below, and *A. parviflora*, abbreviated as R2 below), and sensitive (*A. pacificum*, abbreviated as S below).

The morphology of the lower epidermal trichome under the leaves of the three species were found to be quite different

through leaf SEM (Fig. 2). R1 trichomes were long and fine 'T'-shaped (Fig. 2a), while S was short and broad 'T'-shaped (Fig. 2c). The trichomes of R2 were mostly 'V'-shaped (Fig. 2b). To determine if the observed CRG resistance phenotype was associated with trichome density, we quantified trichomes on the leaves of R and S. The comparison of trichome density showed that the density of trichome under the leaves of S was 6.2/mm², while the density of trichome under R1 was as high as 29.21/mm², 4.71 times higher than that of S, and the density of trichome on the leaves of the plants was negatively correlated with the DSI with a correlation coefficient of -0.998^* (Fig. 3f). In

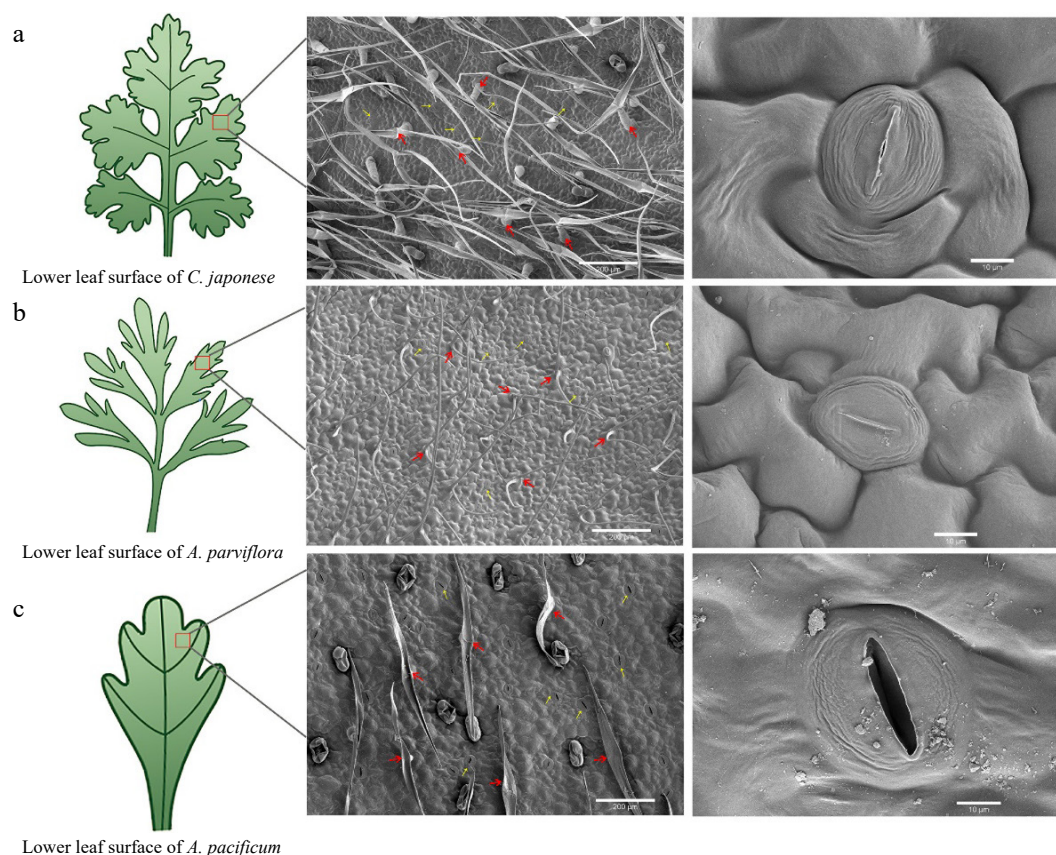


Fig. 2 Scanning electron microscopy (SEM) images of the lower epidermis of leaves from disease-resistant and susceptible materials. From left to right, the parts that were observed under the scanning electron microscope (red box part) showed the distribution and shape of trichome and stomata respectively. The red arrows indicate epidermal hairs, and the yellow arrows point to the stomata.

short, the higher the density of plant trichomes, the greater the resistance to CBS.

Upon further analysis of the stomata, there were marked differences in the stomatal aperture, size and density of the three plants (Fig. 3). To quantify the degree of stomatal closure, we expressed it in terms of stomatal aperture, which was calculated as the ratio of stomatal width to length. The stomata of S were mostly open, while the stomata of R1 were largely closed (Fig. 2, Fig. 3d). Additionally, the stomatal length and width of S were significantly greater than R1 and R2 (Fig. 3c). In addition, we found differences in stomatal density across species (Fig. 3b), but no clear correlation with plant resistance.

The next question we wished to address was to understand whether plant wax content was related to resistance. Wax content was significantly different in species with different resistance levels (Fig. 3e). R1 had the highest wax content at 28.6 mg/g, whereas S leaves had the lowest at 9.4 mg/g, resulting in a 3.04-fold difference between the two.

Differences of volatile metabolites in leaves of disease-resistant germplasm and sensitive germplasm

To further explore the chemical defense mechanism of resistant and sensitive materials, the antifungal activity of plant leaf extracts was determined by plate inhibition test. The results of the experiments were calculated after 4 d of treatment. We found that *A. alternata* grew significantly more on PDA without leaf extract (Fig. 4). Overall, the fungal inhibition effect of the resistant material was better than that of the susceptible

material, although the inhibition rate did not have a regular correlation with the DSI. Unexpectedly, the inhibitory effect of R2 leaf extracts was significantly higher than that of R1.

Encouraged by the divergence *in vitro* antifungal effect, the key antifungal substances were explored. Therefore, GC-MS was used to analyze the composition of VOCs. The retention times for each compound separated by GC-MS were showed in Supplemental Table S2, heat map of the VOCs *via* GC-MS are shown in Fig. 5. Among the three species, 36 kinds of terpenes were detected, the main components were monoterpenes and sesquiterpenes (Fig. 5b). In terms of the content of VOCs in leaves, the highest concentration was found in sesquiterpenes. Furthermore, unlike the other two species, R2 exhibited a very low content of monoterpenes, while other organic volatiles were relatively high; with faltarinol being the main component (Fig. 5c).

The study found that disease-resistant material had significantly higher terpenoid content than disease-susceptible material (Fig. 6a). Beta-Ylangene, beta-Copaene, Germacrene D, gamma-murolene and neophytadiene were present in all three materials with relatively high content. Additionally, analysis demonstrated a positive correlation between the content of these substances and plant disease resistance (Fig. 6g). Interestingly, our experimental materials contained abundant amounts of faltarinol and Germacrene D, which had been identified as antifungal substances^[29, 30].

Considering that the content of Germacrene D was significantly positively correlated with plant resistance, and the relative content of Germacrene D was abundant, we further

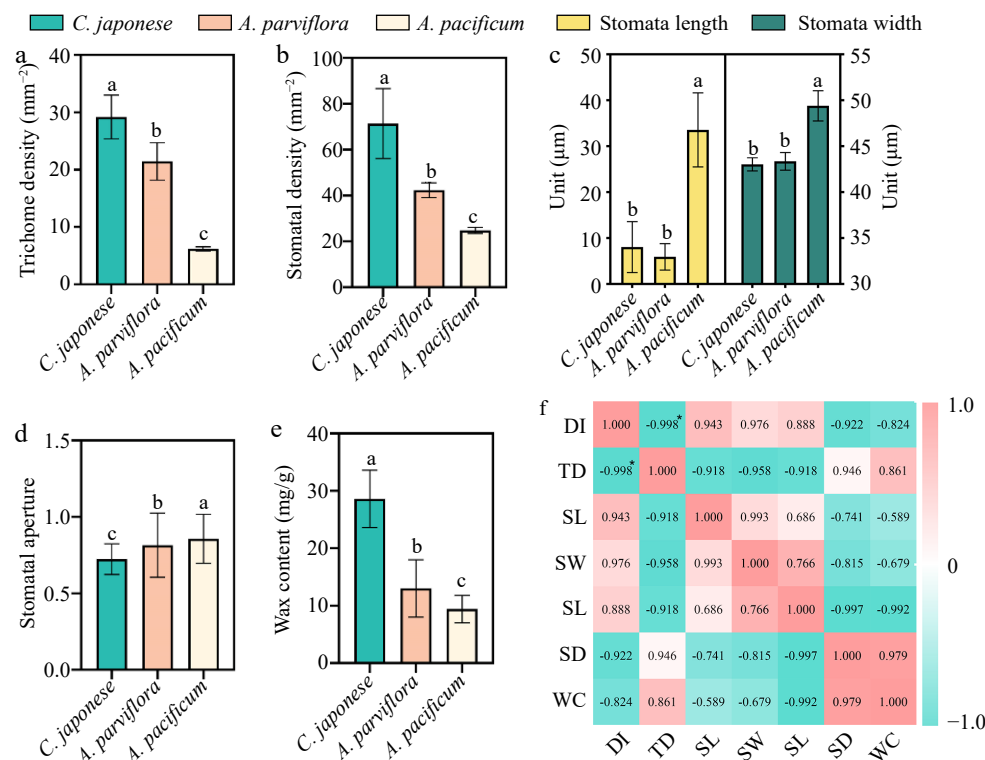


Fig. 3 Correlation analysis of leaf wax content and lower epidermal structure with disease index. (a) Trichome densities of leaf abaxial surfaces, n = 30. (b) Stomata length and width of leaf abaxial surfaces, n = 30. (c) Stomata aperture, n = 30. (d) Stomata densities of leaf abaxial surfaces, n = 30. (e) Wax content of leaves, n = 20. (f) Visualization of the correlation analysis, Pearson correlation coefficient. All bar charts show mean \pm SD. Red and green represent positive and negative correlations, respectively, and color intensity reflects the magnitude of the correlation. DI refers to disease index; TD refers to trichome density; SL refers to stomata length; SW refers to stomata width; SA refers to stomata aperture; SD refers to stomata density; WC refers to wax content.

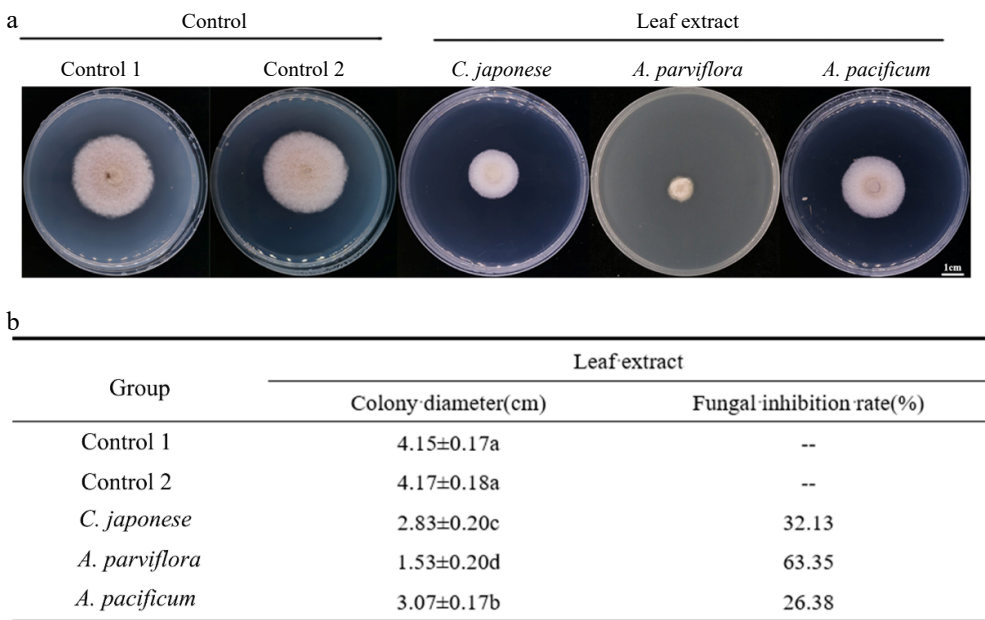


Fig. 4 Antifungal activity of leaf extracts against *A. alternata*. (a) The morphology of the colony on the PDA medium after the leaves extracts were co-cultured with the *A. alternata* for 4 d. (b) Antifungal rate statistics.

analyzed the antifungal activity of Germacrene D, and found that it can significantly inhibit the mycelia growth of *A. alternata* (Fig. 7). Therefore, we hypothesise that the strength of

plant disease resistance is influenced by the terpene content in the leaves, and that an abundance of terpenes contributes to the ability of the plant to fight off invading pathogens.

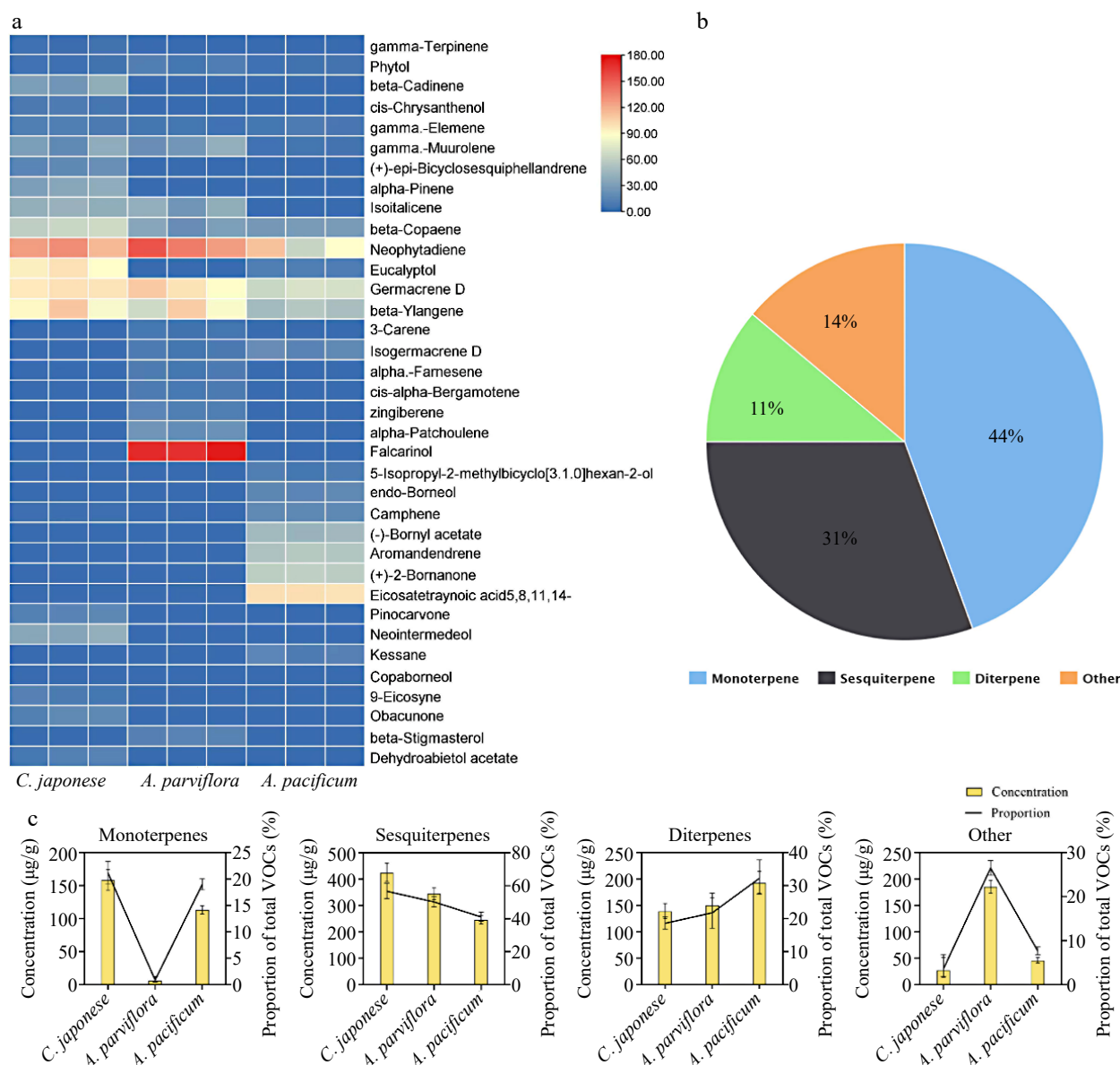


Fig. 5 VOCs components identification of leaf extracts. (a) Heat map with major VOCs (above 1% of total VOCs present in chromatograms) emitted by three species of CRG. Colors reflect the VOC's relative content, $n = 3$. (b) Venn diagram of the proportion of different classes of terpenes. (c) Statistics of different types of VOCs content in the leaves and the proportion of total VOCs content in the leaves.

Discussion

Chrysanthemum-related genera responded differently to simulated disease stress

Excavation of high-quality germplasm resources of wild relatives is an important way to breed chrysanthemums for disease resistance. It was found that the progeny of crosses between cultivated chrysanthemums and *Artemisia* spp. had better black spot resistance than their parents^[31, 32]. In addition, grafting through superior germplasm as rootstocks has become a common and effective method of improving disease resistance in crops^[33]. The resistant germplasm screened by this experiment can be used as hybrid parent or grafting stock for resistance improvement of the chrysanthemum in the future. However, when encountering large quantities of germplasm resources, the problem of accurately and efficiently screening

germplasm resources without destroying them is a problem that remains to be overcome. Detached leaf inoculation assays were used to determine plant germplasm resistance to diseases, such as soybean germplasm for resistance to *Phagophora pachyrhizi*^[34], tomato germplasm resistance to late blight^[35], apple genotypes resistance to *Alternaria* blotch^[36] and oat (*Avena sterilis*) resistance to crown rust^[37]. Among the whole-plant and exfoliated leaf screening techniques for the identification of anthracnose resistance in strawberry plants, scholars noted that the study was used to develop an exfoliated leaf curation method for strawberries that can reliably and rapidly determine the degree of resistance of strawberry germplasm to anthracnose^[38]. We discovered that two inoculation methods showed largely consistent results and that they both reflected the differences in disease resistance between the different materials. This means that the isolated leaf method can be

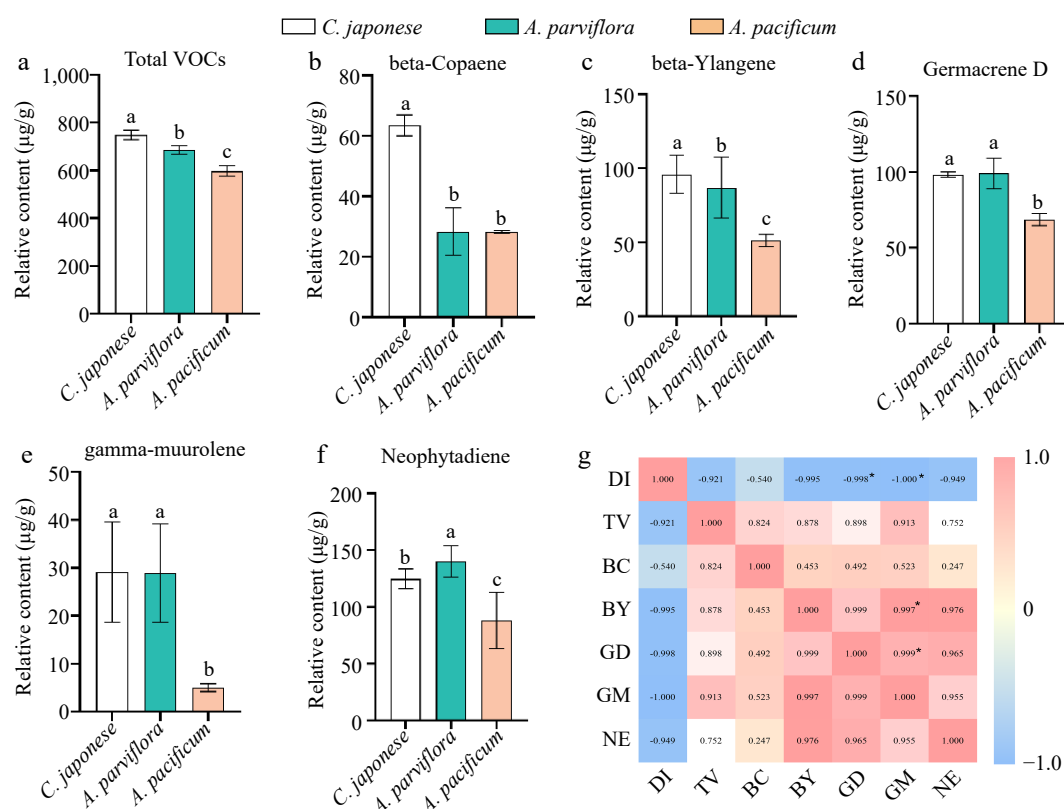


Fig. 6 The contents of volatiles in leaves of different germplasm were significantly different and correlated with plant disease index. (a) Comparison of total volatiles content in leaves. (b)–(f) Comparison of the contents of main volatiles in leaves of different species. (g) Visualization of the correlation analysis, Pearson correlation coefficient. Red and blue represent positive and negative correlations, respectively, and color intensity reflects the magnitude of the correlation. DI refers to disease index, TV refers to total VOCs, BC refers to beta-Copaene, BY refers to beta-Ylangene, GD refers to Germacrene D, GM refers to gamma-murolene, NE refers to neophytadiene.

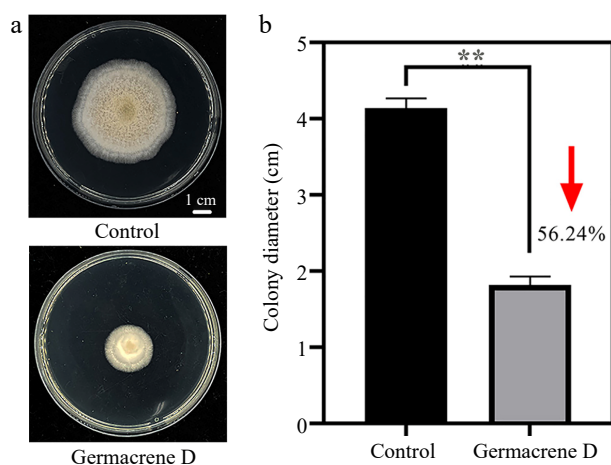


Fig. 7 Inhibition of hyphae growth of *A. alternata* by Germacrene D reagent. (a) The morphology of the colony on the PDA medium after 7 d. (b) Statistical difference of colony growth diameter between control and treatment.

prioritized for primary screening when screening germplasm resources in large quantities in the future, which will effectively reduce the workload. Furthermore, screening for CBS resistance using isolated chrysanthemum leaves is an alternative to inoculating whole plants and may eliminate damage to the desired germplasm.

The association between leaf surface features and disease tolerance

The trichome of plants not only increases the thickness of the epidermis but also behaves as a physical barrier against external invasion. The results of this study showed that the species with the highest trichome height were also the most resistant, in agreement with Patil et al. findings^[39]. At the same time, R had the highest density of trichomes, and the large number of trichomes enriched on the surface of the plant leaves did not facilitate the invasion of the pathogens and thus reduced the disease of the plant, which has also been investigated in other species^[40]. For example, highly resistant grapes had more trichomes and thicker cuticles on the leaves than susceptible germplasm^[41], and in a study of resistance to the fungus *Didymella bryoniae* in Cucurbitaceae, it was found that the higher the density of leaf trichomes, the smaller the average leaf necrosis area^[42]. However, based on phylogenetic statistics, the severity of Asteraceae powdery mildews is not related to trichome density^[43]. In summary, the relationship between trichomes and plant resistance might be related to plant species, pathogen species, and mode of invasion.

It is worth noting that the stomatal length, width, and aperture of susceptible materials are much larger than those of resistant varieties. Stomata are natural openings through which many pathogenic fungi enter plants and the outside world, and their closure is the pivotal line of defense against plant

pathogens^[44, 45]. These findings suggest that the larger size of stomata and bigger stomata aperture are more conducive to pathogen invasion. Although previous studies have shown that stomatal density is related to plant disease resistance^[46], this study did not find a clear regularity between resistance and stomatal density, consistent with Yang et al.^[47].

Waxes played a critical role in resisting infestation by bacterial and fungal pathogens^[48]. Tian et al. showed that the wax layer was a powerful physical structural barrier for plants to resist and delay invasion by pathogenic fungi and that the wax content and trichome density of bitter melon leaves can be used as reference indicators for the identification of resistance to powdery mildew in bitter melon^[49]. Equally, in this experiment, the wax content of R1 was found to be 3.04 times higher than that of S. That means the wax content of the resistant material was higher than that of the disease susceptible material. Combining the leaf trichome and wax content, it could be assumed that the physical defense of the leaf played an outstanding role in the resistance of *C. japonese* to pathogenic infestation.

The association between leaf volatile components and plant tolerance

Plants respond to pathogenic infestation by releasing high amounts of VOCs, which can either serve as a direct defense against pathogens or as a signal for an antimicrobial response. According to several studies, there was a link between plant VOCs^[50] release and resistant plant strains. Grapevine genotypes were resistant to grapevine downy mildew release more monoterpenes and sesquiterpenes than sensitive genotypes^[51]. Additionally, we discovered that the composition and the number of VOCs from plant leaves varied significantly across the range of resistance. Furthermore, different species *in vitro* antifungal activity of *A. alternata* varies, which may be connected to the part of key antifungal substances.

Moreover, another important finding was that the R2 has a significant inhibitory effect compared to others. It is noteworthy that the relative contents of Germacrene D and falcariol in the leaf VOCs of R2 were high. It had been found that big root geranium was associated with the defense mechanism of cashew (*Anacardium occidentale*) leaves in response to invasion by the black mold fungus *Pilgeriella anacardii* Arx & Müller^[52]. Germacrene D was a signal molecule that inhibits the spread of *Phytophthora* from necrotic parts of poplar bark to healthy living tissue^[53]. In strawberry fruit, methyl jasmonate (MeJA) improved resistance to grey mold infection by inducing *FaTPS1* expression and rapidly increasing terpene content, particularly Germacrene D^[54]. In addition, *Pinus nigra* volatile oil rich in terpenoids (Germacrene D-4-ol) and structurally similar terpenoids (Germacrene D) had inhibitory effects against *Aspergillus niger* and *Bacillus subtilis*^[55]. Falcariol was thought to act as a plant chemical defense agent to thwart infection by devastating pathogens^[56]. Falcariol was also beneficial to human health because of its outstanding pharmacological effects^[57–59]. In addition, falcariol has excellent antioxidant activity and antibacterial activity^[60]. Based on the evidence from this work, it would be seen that Germacrene D and falcariol, which had antifungal activity in R2, might play a direct defense role in response to *A. alternata* mycelial invasion.

Over a long period of evolution, plants have developed complex disease-resistance mechanisms to resist pathogenic fungi. The organic extracts of S leaves were relatively effective in this study, but S showed weak resistance to the disease when identified by artificial inoculation. This might be due to deficiencies in physical defense, sparse epidermal hairs, larger stomata, and few wax contents, which facilitate the invasion of mycelium. On the contrary, the leaf surface structure of disease-resistant materials and its antifungal volatile metabolites play a key role in resisting pathogen infection.

Conclusions

In this study, we compared the resistance of 14 species of Chrysanthemum-related genera to Chrysanthemum black spot disease and found that the inoculation of detached leaves can be used as a favorable adjunct to the primary resistance screening of germplasm resources. At the same time, we analyzed the physical and chemical defense mechanisms of disease-resistant and susceptible species. The superior tolerance of *C. japonese* was likely related to its physical defense, a combination of its trichome layer, its closure of stomata, and its abundant wax content, which reduced the invasion of pathogens. In contrast, the tolerance of *A. parviflora* was due to the prominent role of its chemical defense, its high relative content of VOCs substances in the leaves, and its significant fungi inhibitory effect, of which two substances, Germacrene D and falcariol, might be the crucial inhibitory substances. The density of the leaf trichome and the wax content can be used as reference indicators for the identification of resistance to CBS in CRG. The resistance of CRG to the CBS can be partly explained by differences in physical and chemical defenses. The evaluation of the disease tolerance of the CRG further enriched the disease tolerance germplasm resource bank of the chrysanthemum and clarified the different physical and chemical responses of three chrysanthemum-related genera with great differences in disease tolerance, and it has certain reference significance for the research of chrysanthemum disease resistance mechanism.

Author contributions

The authors confirm contribution to the paper as follows: study conception and design: Guan Z, Liu Y; data collection: Zhan Q, Li W; analysis and interpretation of results: Zhao S, Chen S, Fang W, Chen F; draft manuscript preparation: Zhan Q. All authors reviewed the results and approved the final version of the manuscript.

Data availability

All data generated or analyzed during this study are included in this published article and its supplementary information files.

Acknowledgments

This work was supported by grants from the National Natural Science Foundation of China (32171854), the Jiangsu seed industry revitalization project [JBGS (2021) 094] and the Jiangsu Forestry Science and Technology Innovation and Promotion Project [LYKJ(2021)13].

Conflict of interest

The authors declare that they have no conflict of interest. Sumei Chen is the Editorial Board member of *Ornamental Plant Research* who was blinded from reviewing or making decisions on the manuscript. The article was subject to the journal's standard procedures, with peer-review handled independently of this Editorial Board member and the research groups.

Supplementary information accompanies this paper at (<https://www.maxapress.com/article/doi/10.48130/opr-0023-0023>)

Dates

Received 6 November 2023; Revised 6 December 2023; Accepted 15 December 2023; Published online 9 January 2024

References

- Calone R, Bregaglio S, Sanoubar R, Noli E, Lambertini C, et al. 2021. Physiological adaptation to water salinity in six wild halophytes suitable for mediterranean agriculture. *Plants* 10:309
- Guan Z, Chen S, Wang Y, Chen F. 2010. Screening of salt-tolerance concentration and comparison of salt-tolerance for chrysanthemum and its related taxa. *Chinese Journal of Ecology* 29:467–72
- Chen J, Zhao X, Zhang Y, Li Y, Luo Y, et al. 2019. Effects of drought and rehydration on the physiological responses of *Artemisia halodendron*. *Water* 11:793
- Liu H, Wang Q, Wang J, Liu Y, Renzeng W, et al. 2022. Key factors for differential drought tolerance in two contrasting wild materials of *Artemisia wellbyi* identified using comparative transcriptomics. *BMC Plant Biology* 22:445
- Yin D, Chen S, Chen F, Guan Z, Fang W. 2009. Morphological and physiological responses of two chrysanthemum cultivars differing in their tolerance to waterlogging. *Environmental and Experimental Botany* 67:87–93
- Alhaithloul HAS. 2019. Impact of combined heat and drought stress on the potential growth responses of the desert grass *Artemisia sieberi alba*: relation to biochemical and molecular adaptation. *Plants* 8:416
- Rebbi AEM, Lounici H, Lahrech MB, Morel JL. 2019. Response of *Artemisia herba alba* to hexavalent chromium pollution under arid and semi-arid conditions. *International Journal of Phytoremediation* 21:224–29
- Zhang X, Sun X, Zhang S, Yang J, Liu F, et al. 2019. Comprehensive transcriptome analysis of grafting onto *Artemisia scoparia* W. to affect the aphid resistance of chrysanthemum (*Chrysanthemum morifolium* T.). *BMC Genomics* 20:776
- Guetat A, Al-Ghamdi FA, Osman AK. 2017. The genus *Artemisia* L. in the northern region of Saudi Arabia: essential oil variability and antibacterial activities. *Natural Product Research* 31:598–603
- Mamatova AS, Korona-Glowniak I, Skalicka-Woźniak K, Józefczyk A, et al. 2019. Phytochemical composition of wormwood (*Artemisia gmelinii*) extracts in respect of their antimicrobial activity. *BMC Complementary and Alternative Medicine* 19:288
- Zhang Y, Song H, Wang X, Zhou X, Zhang K, et al. 2020. The roles of different types of trichomes in tomato resistance to cold, drought, whiteflies, and *Botrytis*. *Agronomy* 10:411
- Kärklīņa K, Lācis G, Lāce B. 2021. Differences in leaf morphological parameters of pear (*Pyrus communis* L.) based on their susceptibility to european pear rust caused by *Gymnosporangium sabinae* (Dicks.) Oerst. *Plants* 10:1024
- Tateda C, Obara K, Abe Y, Sekine R, Nekoduka S, et al. 2019. The host stomatal density determines resistance to *Septoria gentianae* in Japanese Gentian. *Molecular Plant-Microbe Interactions* 32:428–36
- Crowell CR, Bekauri MM, Cala AR, McMullen P, Smart LB, et al. 2020. Differential susceptibility of diverse *Salix* spp. to *Melampsora americana* and *Melampsora paradoxa*. *Plant Disease* 104:2949–57
- Li J, Zhang C, Zhang Y, Gao H, Wang H, et al. 2022. An apple long-chain acyl-CoA synthase, *MdLACS1*, enhances biotic and abiotic stress resistance in plants. *Plant Physiology and Biochemistry* 189:115–25
- Zhang Y, Zhang C, Wang G, Wang Y, Qi C, et al. 2019. The R2R3 MYB transcription factor MdMYB30 modulates plant resistance against pathogens by regulating cuticular wax biosynthesis. *BMC Plant Biology* 19:362
- Zhu J, Huang K, Cheng D, Zhang C, Li R, et al. 2022. Characterization of cuticular wax in tea plant and its modification in response to low temperature. *Journal of Agricultural and Food Chemistry* 70:13849–61
- Lewandowska M, Keyl A, Feussner I. 2020. Wax biosynthesis in response to danger: its regulation upon abiotic and biotic stress. *New Phytologist* 227:698–713
- Bourgau F, Gravot A, Milesi S, Gontier E. 2001. Production of plant secondary metabolites: a historical perspective. *Plant Science* 161:839–51
- Li C, Leopold AL, Sander GW, Shanks JV, Zhao L, et al. 2013. The ORCA2 transcription factor plays a key role in regulation of the terpenoid indole alkaloid pathway. *BMC Plant Biology* 13:155
- Ritala A, Dong LM, Imseng N, Seppänen-Laakso T, Vasilev N, et al. 2014. Evaluation of tobacco (*Nicotiana tabacum* L. cv. Petit Havana SR1) hairy roots for the production of geraniol, the first committed step in terpenoid indole alkaloid pathway. *Journal of Biotechnology* 176:20–28
- Stitt M, Sulpice R, Keurentjes J. 2010. Metabolic networks: how to identify key components in the regulation of metabolism and growth. *Plant Physiology* 152:428–44
- Xue H, Jiang Y, Zhao H, Köllner TG, Chen S, et al. 2019. Characterization of composition and antifungal properties of leaf secondary metabolites from thirteen cultivars of *Chrysanthemum morifolium* Ramat. *Molecules* 24:4202
- Li H, Liu Y, Chen S, Jiang J, Song A, et al. 2020. Variation for resistance to *Alternaria tenuissima* and potential structural mechanism among different cultivars of *Chrysanthemum morifolium*. *Phyton-International Journal of Experimental Botany* 89:851–59
- He X, Jiang Y, Chen S, Chen F, Chen F. 2023. Terpenoids and their possible role in defense against a fungal pathogen *Alternaria tenuissima* in *Chrysanthemum morifolium* cultivars. *Journal of Plant Growth Regulation* 42:1144–57
- Liu L, Chen F, Chen S, Fang W, Liu Y, et al. 2021. Dual species dynamic transcripts reveal the interaction mechanisms between *Chrysanthemum morifolium* and *Alternaria alternata*. *BMC Genomics* 22:523
- Liu Y, Xin J, Liu L, Song A, Guan Z, et al. 2020. A temporal gene expression map of Chrysanthemum leaves infected with *Alternaria alternata* reveals different stages of defense mechanisms. *Horticulture Research* 7:23
- Guan Y, He X, Wen D, Chen S, Chen F, et al. 2022. *Fusarium oxysporum* infection on root elicit aboveground terpene production and salicylic acid accumulation in *Chrysanthemum morifolium*. *Plant Physiology and Biochemistry* 190:11–23
- Merad N, Andreu V, Chaib S, de Carvalho Augusto R, Duval D, et al. 2021. Essential oils from two apiaceae species as potential agents in organic crops protection. *Antibiotics* 10:636
- Ruiz-Vásquez L, Ruiz Mesia L, Caballero Ceferino HD, Ruiz Mesia W, Andrés MF, et al. 2022. Antifungal and herbicidal potential of *Piper* essential oils from the Peruvian Amazonia. *Plants* 11:1793
- Zhu W, Zhang F, Chen S, Xu L, Wang L, et al. 2014. Intergeneric hybrids between *Chrysanthemum morifolium* 'Nannongxiaoli' and *Artemisia vulgaris* 'Variegata' show enhanced resistance against both aphids and *Alternaria* leaf spot. *Euphytica* 197:399–408

32. Deng Y, Chen S, Chang Q, Wang H, Chen F. 2012. The chrysanthemum \times *Artemisia vulgaris* intergeneric hybrid has better rooting ability and higher resistance to alternaria leaf spot than its chrysanthemum parent. *Scientia Horticulturae* 134:185–90
33. Smith J, Saravanakumar D. 2022. Development of resistance in tomato plants grafted onto *Solanum torvum* against bacterial wilt disease. *Journal of Plant Diseases and Protection* 129:1389–99
34. Paul C, Motter HZ, Walker DR. 2020. Reactions of soybean germplasm accessions to six *Phakopsora pachyrhizi* isolates from the United States. *Plant Disease* 104:1087–95
35. Foolad MR, Sullenberger MT, Ashrafi H. 2015. Detached-leaflet evaluation of tomato germplasm for late blight resistance and its correspondence to field and greenhouse screenings. *Plant Disease* 99:718–22
36. Abe K, Iwanami H, Kotoda N, Moriya S, Takahashi Sumiyoshi S. 2010. Evaluation of apple genotypes and *Malus* species for resistance to Alternaria blotch caused by *Alternaria alternata* apple pathotype using detached-leaf method. *Plant Breeding* 129:208–18
37. Paczos-Grzęda E, Sowa S, Boczkowska M, Langdon T. 2019. Detached leaf assays for resistance to crown rust reveal diversity within populations of *Avena sterilis*. *Plant Disease* 103:832–40
38. Miller-Butler MA, Smith BJ, Babiker EM, Kreiser BR, Blythe EK. 2018. Comparison of whole plant and detached leaf screening techniques for identifying anthracnose resistance in strawberry plants. *Plant Disease* 102:2112–19
39. Patil PG, Shashidhar HE, Byregowda M, Reena GAM, Ashok TH, et al. 2017. Association of leaf micro-morphological features with serility mosaic disease resistance in pigeonpea. *Journal of Environmental Biology* 38:649–56
40. Kono A, Shimizu T. 2020. Leaf trichomes as an effective structure for disease resistance: the case of grapevine downy mildew. *Japan Agricultural Research Quarterly* 54:293–98
41. Hou X, Zhang G, Han R, Wan R, Li Z, et al. 2022. Ultrastructural observations of *Botrytis cinerea* and physical changes in resistant and susceptible grapevines. *Phytopathology* 112:387–95
42. Rennberger G, Keinath AP, Hess M. 2017. Correlation of trichome density and length and polyphenol fluorescence with susceptibility of five cucurbits to *Didymella bryoniae*. *Journal of Plant Diseases and Protection* 124:313–18
43. Bradshaw M, Goolsby E, Mason C, Tobin PC. 2021. Evolution of disease severity and susceptibility in the Asteraceae to the powdery mildew *Golovinomyces latiporus*: major phylogenetic structure coupled with highly variable disease severity at fine scales. *Plant Disease* 105:268–75
44. Li X, Rengel Z, Chen Q. 2022. Phytomelatonin prevents bacterial invasion during nighttime. *Trends in Plant Science* 27:331–34
45. Luiz C, Caires NP, de Aguiar T, Blainski JML, da Silva Behs J, et al. 2022. Resistance of strawberries to *Xanthomonas fragariae* induced by aloe polysaccharides and essential oils nanoemulsions is associated with phenolic metabolism and stomata closure. *Australasian Plant Pathology* 51:305–14
46. Dutton C, Hórák H, Hepworth C, Mitchell A, Ton J, et al. 2019. Bacterial infection systemically suppresses stomatal density. *Plant, Cell & Environment* 42:2411–21
47. Yang H, Han S, He D, Jiang S, Cao G, et al. 2021. Resistance evaluation of walnut (*Juglans* spp.) against *Xanthomonas arboricola* and the correlation between leaf structure and resistance. *Forest Pathology* 51:e12659
48. Ziv C, Zhao ZZ, Gao YG, Xia Y. 2018. Multifunctional roles of plant cuticle during plant-pathogen interactions. *Frontiers in Plant Science* 9:1088
49. Tian L, Shang S, Yang Y, Si L, Li D. 2013. Relationship between the leaf structure of bitter melon and resistance to powdery mildew. *Acta Botanica Boreali-Occidentalia Sinica* 33:2010–15
50. Hammerbacher A, Coutinho TA, Gershenzon J. 2019. Roles of plant volatiles in defence against microbial pathogens and microbial exploitation of volatiles. *Plant, Cell & Environment* 42:2827–43
51. Alarcon AA, Lazazzara V, Cappellin L, Bianchedi PL, Schuhmacher R, et al. 2015. Emission of volatile sesquiterpenes and monoterpenes in grapevine genotypes following *Plasmopara viticola* inoculation in vitro. *Journal of Mass Spectrometry* 50:1013–22
52. de Sousa DB, Da Silva GS, Guedes JAC, Serrano LAL, Martins MVV, et al. 2022. Volatile metabolomics from cashew leaves: assessment of resistance biomarkers associated with black mold (*Pilgeriella anacardii* Arx & Müller). *Journal of the Brazilian Chemical Society* 33:1423–40
53. Đurković J, Bubeníková T, Gužmerová A, Fleischer P, Kurjak D, et al. 2021. Effects of *Phytophthora* inoculations on photosynthetic behaviour and induced defence responses of plant volatiles in field-grown hybrid poplar tolerant to bark canker disease. *Journal of Fungi* 7:969
54. Zhang Z, Lu S, Yu W, Ehsan S, Zhang Y, et al. 2022. Jasmonate increases terpene synthase expression, leading to strawberry resistance to *Botrytis cinerea* infection. *Plant Cell Reports* 41:1243–60
55. Šarac Z, Matejić JS, Stojanović-Radić ZZ, Veselinović JB, Džamić AM, et al. 2014. Biological activity of *Pinus nigra* terpenes—Evaluation of FtsZ inhibition by selected compounds as contribution to their antimicrobial activity. *Computers in Biology and Medicine* 54:72–8
56. Santos P, Busta L, Yim WC, Cahoon EB, Kosma DK. 2022. Structural diversity, biosynthesis, and function of plant falcarin-type polyacetylenic lipids. *Journal of Experimental Botany* 73:2889–904
57. Dawid C, Dunemann F, Schwab W, Nothnagel T, Hofmann T. 2015. Bioactive C₁₇-polyacetylenes in carrots (*Daucus carota* L.): current knowledge and future perspectives. *Journal of Agricultural and Food Chemistry* 63:9211–22
58. Hou JH, Shin H, Jang KH, Park CK, Koo B, et al. 2019. Anti-acne properties of hydrophobic fraction of red ginseng (*Panax ginseng* C.A. Meyer) and its active components. *Phytotherapy Research* 33:584–90
59. Kobaek-Larsen M, El-Houri RB, Christensen LP, Al-Najami I, Fretté X, et al. 2017. Dietary polyacetylenes, falcarinol and falcariindiol, isolated from carrots prevents the formation of neoplastic lesions in the colon of azoxymethane-induced rats. *Food & Function* 8:964–74
60. Medbouhi A, Merad N, Khadir A, Bendahou M, Djabou N, et al. 2018. Chemical composition and biological investigations of *Eryngium triquetrum* essential oil from Algeria. *Chemistry & Biodiversity* 15:e1700343



Copyright: © 2024 by the author(s). Published by Maximum Academic Press, Fayetteville, GA. This article is an open access article distributed under Creative Commons Attribution License (CC BY 4.0), visit <https://creativecommons.org/licenses/by/4.0/>.